# Formation of $BaSO_4$ Fibres with Morphological Complexity in Aqueous Polymer Solutions

**Limin Qi,[a] Helmut Cölfen,*[a] Markus Antonietti,[a] Mei Li,[b] Jeremy D. Hopwood,[b] Alexandra J. Ashley,[b] and Stephen Mann*[b]**

**Abstract:** $BaSO_4$ fibres with morphological complexity were formed in aqueous solution with polyacrylate and partially monophosphonated poly(ethyleneoxide)-block-poly(methacrylic acid) additives by a simple precipitation reaction. For polyacrylate, formation of the fibrous deposits was strongly dependent on the level of supersaturation (S) and $Ba^{2+}$:polymer molar ratio (R). At $S = 60$ to 80, and $R = 3$ to 14, highly anisotropic crystalline fibres consisting of bundles of $BaSO_4$ nanofilaments were formed after several weeks, although the yield was low. The nanofilaments were also organized into cone-shaped aggregates at $S = 80$, and at lower R values these formed higher-order structures that consisted of multiple cone-on-cone assemblies with remarkable self-similarity. Increasing the supersaturation produced ovoid or cross-shaped dendritic particles for the range of molar ratios studied. In contrast, $BaSO_4$ crystallisation in the presence of a partially phosphonated block copolymer gave a high yield of $BaSO_4$ fibres up to 100 μm in length, and consisting of co-aligned bundles of 30 nm-diameter defect-free single-crystal nanofilaments with a uniform growth tip. A model for the defect-free growth of $BaSO_4$ nanofilaments in aqueous polymer solutions based on amorphous precursor particles, vectorially directing forces and van der Waals attraction is proposed.

**Keywords:** aggregation · barium · crystal growth · morphogenesis · polymers

## Introduction

Recently, much effort has been devoted to the controlled synthesis of one-dimensional nanostructured materials, such as nanofibres (nanowires or nanorods) and nanotubes, due to their fundamental and technological importance.[1–5] Although many effective methods have been developed to prepare nanowires or nanorods of a variety of inorganic materials including semiconductors,[1–3, 6–8] metals,[9–11] metal oxides[12] and hydroxides,[13] the facile synthesis of inorganic nanofibres in aqueous solutions at room temperature remains synthetically challenging. Specifically, reverse micelles and microemulsions have been successfully used as organised reaction microenvironments for the controlled synthesis of copper nanorods,[11, 14] or $BaSO_4$,[15] $BaCO_3$[16] and $CaSO_4$[17] nanowires at room temperature. However, there are few reports on the preparation of inorganic nanofibres by using organic templates or additives in aqueous solution at room temperature; an example being the preparation of Au nanorods by using rodlike cationic surfactant micelles as templates.[18, 19]

Interestingly, $BaSO_4$ nanofibres were already observed in aqueous polymer solutions by Brase in 1990,[20] by using copolymers containing polyacrylate and polyvinyl sulfonate domains. Brase pointed out that for fibre formation, the polymer must have a high percentage of carboxy groups, the $BaSO_4$ concentration must be sufficiently high ($> 0.4$ mM) and the concentration of $Ba^{2+}$ ions must be similar to the concentration of polymer subunits. A similar study was undertaken by Benton, Collins and co-workers in 1993,[21] but using polymaleate-based macromolecules. They produced $BaSO_4$ nanofibres by the rapid mixing of brine solutions containing $Ba^{2+}$ and $SO_4^{2-}$ ions at 95 °C using a copolymer with a high content of maleic acid as a crystal growth modifier, and found that the size and arrangement of the fibres depended on the solution pH. Specifically, fibres grown at pH 6 were similar to the fibres observed by Brase and were

[a] Dr. H. Cölfen, Dr. L. Qi,[+] Prof. Dr. M. Antonietti
Max-Planck-Institute of Colloids and Interfaces
Colloid Chemistry
Research Campus Golm, 14424 Potsdam (Germany)
Fax: (+49) 331-5679502
E-mail: Coelfen@mpikg-golm.mpg.de

[b] Prof. Dr. S. Mann, M. Li, Dr. J. D. Hopwood, A. J. Ashley
School of Chemistry
University of Bristol
Bristol BS8 1TS (UK)
Fax. (+44) 117-9251295
E-mail: s.mann@bristol.ac.uk

[+] Present address:
College of Chemistry, Peking University
Beijing 100871 (P. R. China)

  0947-6539/01/0716-3526 $ 17.50+.50/0 

found to be single crystals elongated along the [001] axis. In contrast, fibres grown at pH 5 were smaller in length and were arranged into hollow, cone-like structures (diameter 5–20 μm); moreover, the basal edges of the cones were revealed to be fractal, with smaller cones attached to the edges of the larger cones.

Recently, it has been shown that so-called double-hydrophilic block copolymers[22, 23] can act as effective crystal growth modifiers and exert a strong influence on the external morphology and/or crystalline structure of particles of a variety of inorganic materials such as calcium carbonate,[24–26] calcium phosphate,[27] and barium sulfate.[28, 29] Specifically, we have demonstrated that pure, well-defined bundles of $BaSO_4$ nanofibres can be produced in the presence of the phosphonated copolymer PEG-*b*-PMAA-$PO_3H_2$ by a double-jet precipitation process at room temperature. However, the growth mechanism of the bundles of nanofibres remains to be elucidated.[29] It is worth noting that $BaSO_4$ nanofibres have also been synthesised in reverse microemulsions formulated with the anionic surfactant sodium bis(2-ethyhexyl)sulfosuccinate (Aerosol OT, AOT).[15] A mechanism for the formation of the $BaSO_4$ nanofibres in the microemulsion media was proposed in which the primary surfactant–nanoparticle aggregates were specifically formed by a self-terminating process and evolved into the fibrous structures through structural reconstruction.[30]

Herein, we describe the formation of a variety of complex $BaSO_4$ morphologies, such as bundled fibres, brush-like and cone-shaped structures, and unusual "cone-on-cone" assemblies, in aqueous polyacrylate solutions at room temperature. In each case, the structures consist of co-aligned or divergent arrays of $BaSO_4$ nanofilaments. We also describe a high-yield preparation of $BaSO_4$ bundled fibres in the presence of a phosphonated block copolymer PEG-*b*-PMAA-$PO_3H_2$. The nanofilaments are produced by transformation of amorphous nanoparticles that are present in colloidal aggregates, and which deposit on foreign substrates or surfaces of the reaction vessel. Heterogeneous nucleation and growth process into solution then gives rise to the high anisotropy of the bundled fibres or the divergent cone-shaped structures.

## Results and Discussion

**$BaSO_4$ crystallisation in the presence of sodium polyacrylate**: Precipitation experiments, performed at 0.11 and 0.53 mM sodium polyacrylate ([$BaSO_4$] = 1.0 or 1.5 mM, and 1.5, 2.0 or 2.5 mM, respectively) produced high aspect ratio fibres, 1–30 μm and 10–100 μm in width and length, respectively. In contrast, cross-shaped dendritic crystals were observed in the absence of the polymer. The fibres, which were shown by elemental analysis (EDXA) and electron diffraction analysis to be crystalline barium sulfate (barite) (data not shown), were only identified in scanning electron micrographs in significant numbers after one week so experiments were often left unstirred for two to three weeks. Only non-fibrous crystals (ovoids and cross-shaped dendrites) were observed up to 24 h after mixing the reagents. Optical microscopy of samples examined after several weeks indicated that about 10% of the $BaSO_4$ particles were in the form of fibres.

A clear transition from fibrous to non-fibrous particles was observed with increasing concentration (supersaturation) of barium sulfate (Figure 1). The corresponding morphological

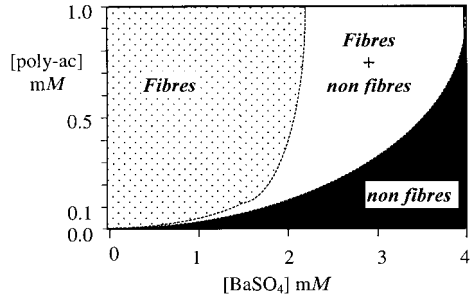


Figure 1. Precipitation diagram for fibrous and non-fibrous particles according to reference [32].

characteristics of the fibrous and non-fibrous forms are summarised in Table 1. The former was present in three distinct morphological types. Firstly, at S = 60 to 80, and a $Ba^{2+}$:polymer molar ratio between 3:1 to 14:1, closely packed, brush-like aggregates of crystalline fibres were produced (Figure 2a).

The strands, which were typically curved along their long axes, were often attached at one end to irregularly shaped particles and when agitated in solution displayed considerable freedom of movement. In many cases, the brush-like structures appeared to have nucleated against a flat surface such as the glass walls of the container (Figures 2a and b), indicating a heterogeneous nucleation and growth process. Higher magnification scanning electron miscroscopy (SEM) images indicated that the individual fibres in the brush-like structures were subdivided into densely packed $BaSO_4$ nanofilaments (Figure 2c). This was confirmed by transmission electron microscopy (TEM) analysis, which showed that the nanofilaments were about 50 nm in width, attached parallel to one another, and continuous along the entire length of the fibres. Significantly, single-crystal electron diffraction patterns were obtained from the nanofilament bundles (Figure 2d), indicating that the nanofilaments in each fibre were crystallographically coherent. Moreover, the electron diffraction patterns showed that the fibres were predominantly aligned along their [010] axis (Figure 2d, inset).

A second morphological type in the form of cone-shaped aggregates (Figure 3) of $BaSO_4$ nanofilaments was also observed along with the brush-like structures at S = 80, but not S = 60. The cones consisted of a divergent array of nanofilaments, arranged radially to form a coherent outer wall and porous internal microstructure with concentric ring-like patterns. Most of the cones were open-ended although a few were sealed with a smooth flat end face.

Increasing the concentration of polymer to 0.53 mM at S = 80 produced higher order structures that consisted of multiple cone-on-cone assemblies with remarkable self-similarity (Figure 4). The multiple cones were attached on average to one cone above and one below. Each cone was hollow, and

  0947-6539/01/0716-3527 $ 17.50+.50/0 

Table 1. Physical characteristics of particles formed in the presence of sodium polyacrylate ($M_n = 5100\ g\,mol^{-1}$). The data is based on optical and scanning-electron microscope observations. The exception being the fibres in sample 7, which were measured by TEM.

| Sample | [Acrylate], mM | [$BaSO_4$] mM | S | Particle shape | Particle size | Yield |
|---|---|---|---|---|---|---|
| 1 | 0 | 1.0 | 60 | cross-shaped dendrites | 20 μm | high |
| 2 | 0 | 10.0 | 270 | cross-shaped dendrites | 16 μm | high |
| 3 | 0.11 | 1.0 | 60 | ***fibrous***; brush-like | brushes: 10 μm long, 1 μm wide | moderate |
| 4 | 0.11 | 1.5 | 80 | ***fibrous***; brush-like | brushes: 25 μm long, 5–10 μm wide<br>strands: 0.4–1.0 μm wide | low |
| | | | | ***fibrous***; cone-shaped | cones: 20–50 μm wide<br>strands: 0.2 μm wide | low |
| | | | | ovoids | 3 μm | high |
| 5 | 0.11 | 2.0 | 90 | irregular ovoid | 1–3 μm | high |
| 6 | 0.11 | 5.0 | 170 | cross-shaped dendrites | 3–4 μm | high |
| 7 | 0.53 | 1.5 | 60 | ***fibrous***; brush-like | brushes: 20–50 μm long, 10–30 μm wide<br>strands: 0.1–0.2 μm wide<br>fibres: 0.03–0.1 μm wide, up to 50 μm long | low |
| 8 | 0.53 | 2.0 | 80 | ***fibrous***; multiple cones | multiple cones: 100 μm long, 15 μm wide<br>strands: 0.2 μm wide | low |
| | | | | ovoids | 4 μm | low |
| 9 | 0.53 | 2.5 | 100 | ***fibrous***; brush-like | brushes: 50 μm long | low |
| | | | | ovoids | 3 μm | low |
| 10 | 0.53 | 5.0 | 170 | cross-shaped dendrites | 1–2 μm | low |
| 11 | 0.53 | 7.5 | 220 | irregular ovoids | 0.5–1 μm | moderate |

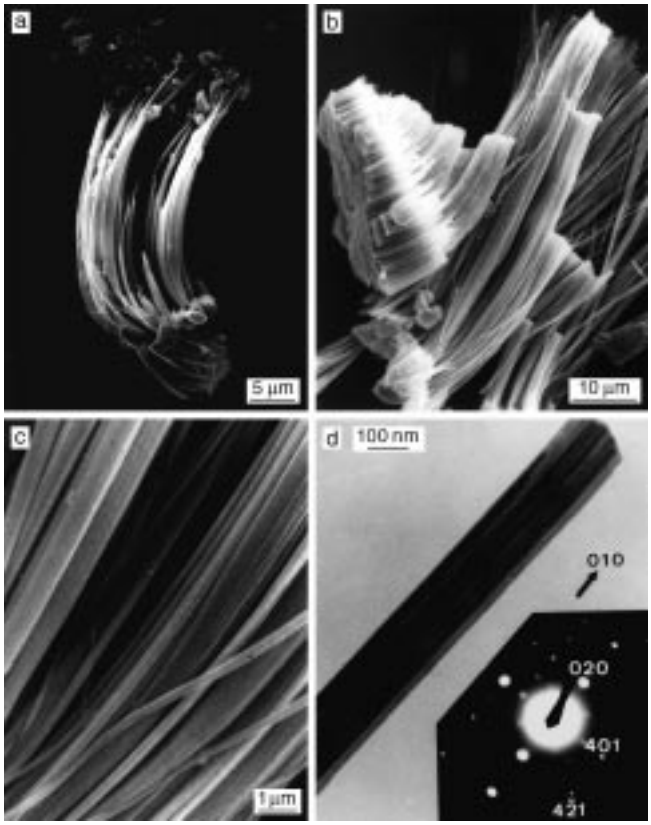


Figure 2. Micrographs of brush-like $BaSO_4$ particles prepared in the presence of poly(acrylate): a) SEM image of sample 4, b,c) SEM image of sample 7, d) TEM image and associated electron diffraction pattern of $BaSO_4$ fibres and strands.

composed of nanofilaments that diverged from the base to produce a densely packed array on the outer surface (Figure 4, inset). For the range of molar ratios studied, increasing the supersaturation above S = 100 produced ovoid or cross-shaped dendritic $BaSO_4$ particles, similar to crystals produced in the absence of the polyacrylate.

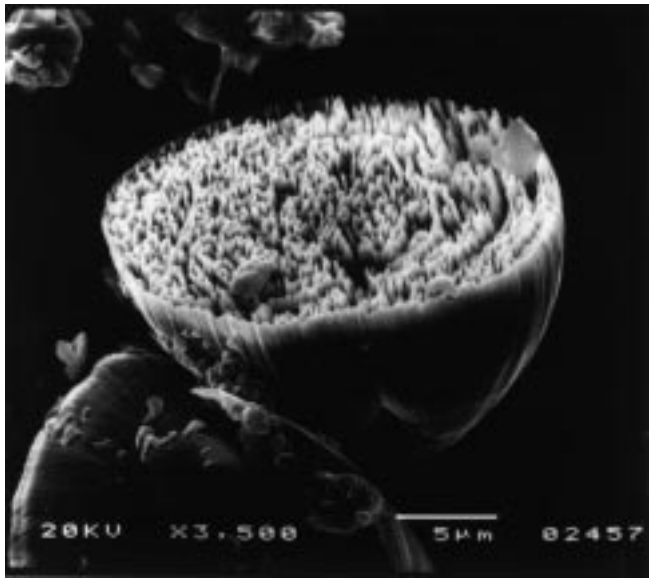


Figure 3. SEM image of cone-shaped $BaSO_4$ particles prepared in the presence of polyacrylate (sample 4). Note the concentric pattern.

**$BaSO_4$ crystallisation in the presence of PEG-*b*-PMAA-$PO_3H_2$**: High yields of bundles of $BaSO_4$ nanofibres were synthesised by successively adding aqueous $SO_4^{2-}$ and $Ba^{2+}$ solutions to an aqueous solution of PEG-*b*-PMAA-$PO_3H_2$ at pH 5 and room temperature. Although the unstirred reaction solution remained transparent for up to four days, a fine white solid gradually appeared on the side and bottom of the glass walls after about 3 h of mixing. Figure 5a shows that the obtained product consisted of large amounts of bundles of $BaSO_4$ fibres up to several hundred micrometers in length,



0947-6539/01/0716-3528 $ 17.50+.50/0 *Chem. Eur. J.* **2001**, *7*, No. 16

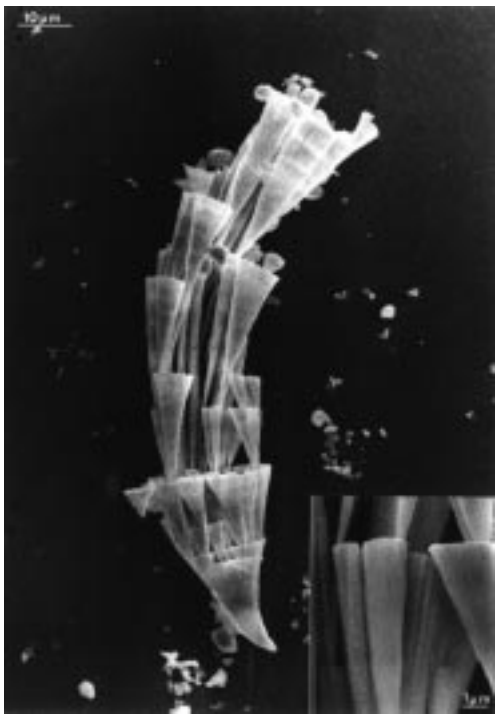

Figure 4. SEM image of a multiple cone-shaped $BaSO_4$ particle prepared in the presence of polyacrylate (sample 8). The inset shows a high magnification image, reavealing the internal arrangement of the strands.

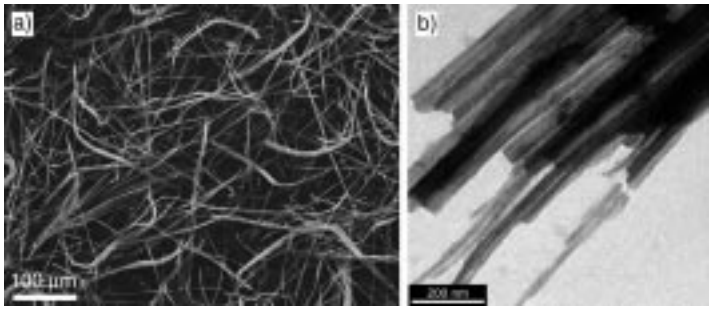


Figure 5. $BaSO_4$ fibres obtained in the presence of PEG-*b*-PMAA-$PO_3H_2$ in glass tubes after one day of mixing.

which appeared to grow from a single growth point. TEM images (e.g. Figure 5b) clearly revealed that the bundles were composed of nanofilaments with uniform diameters (20–30 nm).

The bundles of $BaSO_4$ nanofibres were essentially the same in morphology and structure as those obtained previously by us in the presence of the same copolymer but using a double-jet precipitation process.[29] These fibres consist of single-crystal barite nanofilaments elongated along the crystallographic [1$\bar{2}$0] axis,[29] in contrast to the above results for polyacrylate in which the axis of elongation is [010]. However, the change from the very fast double-jet precipitation in reference [29] to the here applied crystallisation by successive reactant addition in the presence of the same block copolymer did not lead to any observable change. Both procedures yield amorphous nanoparticles in the beginning followed by a slow growth process so that the precipitation speed of the initial particles becomes negligible.

To study the early stages of growth of the fibres formed on the glass walls, samples were collected after one hour of mixing by sonication of the glass tube. The results were also compared with immature crystals observed in situ during heterogeneous nucleation on the carbon support film of TEM copper grids. As shown in Figure 6a, the particles obtained

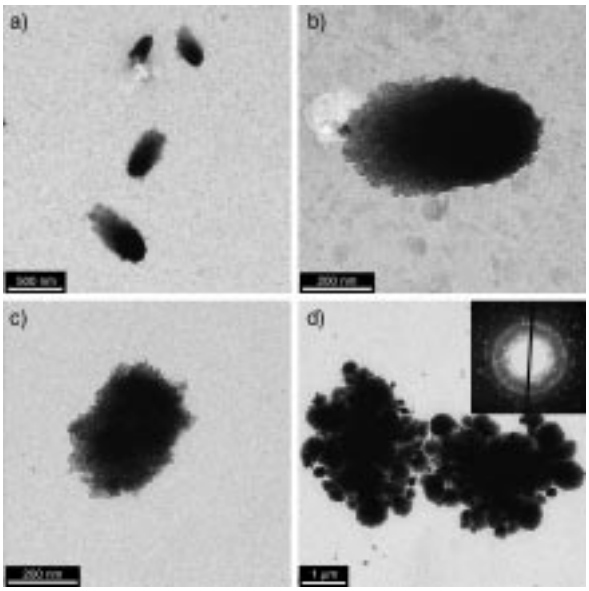


Figure 6. $BaSO_4$ particles obtained in the presence of PEG-*b*-PMAA-$PO_3H_2$ with an ageing time of 1 h: a,b) in glass tubes, and c) on carbon films. d) shows particles obtained after an ageing time of 3 h. Inset of d) shows the corresponding electron diffraction pattern that exhibits sharp spots corresponding to the barite structure.

were 200 to 500 nm in size and exhibited an anisotropic structure that in projection was consistent with a small cone-shaped structure.

The base of the cone was electron dense, whereas the growth edges consisted of a loose aggregate of 25 nm-sized electron dense particles (Figure 6b). Corresponding electron diffraction analysis indicated that the $BaSO_4$ nanoparticles were amorphous. Presumably, the larger anisotropic particles represent the initial nuclei of the mature $BaSO_4$ fibres from which the dense ends of the particles evolve into the starting points of the bundles of $BaSO_4$ nanofilaments after reconstruction and crystallisation under the influence of the phosphonated double-hydrophilic block copolymer.

To directly monitor the heterogeneous nucleation and growth process of the bundles of $BaSO_4$ nanofilaments, samples were prepared on TEM grids coated with a carbon film. Irregular aggregates of $BaSO_4$ nanoparticles with no apparent shape anisotropy were observed on the support film after one hour (Figure 6c). Corresponding electron diffraction analysis indicated that the nanoparticles were amorphous. The results suggest that the aggregates formed on the TEM support film were similar to the slightly anisotropic particles shown in Figures 6a and b, except that they are viewed in situ along their long axis due to heterogeneous nucleation on the carbon support film. After an ageing time of 3 h, outgrowths of nanofilament-containing bundles were observed on the TEM grids. Two large bundles, several

micrometers in diameter, that comprise many smaller bundle-like structures with various sizes can be clearly seen in Figure 6d. The corresponding electron diffraction pattern showed many sharp reflections corresponding to crystalline barite (Figure 6d, inset).

SEM images indicated that the nanofilaments in each bundle were splayed outwards from the centre. The length of the nanofilaments increased significantly and after 24 h large splayed fibres were observed across the TEM grid (Figure 7a). Each fibre exhibited a single starting point and

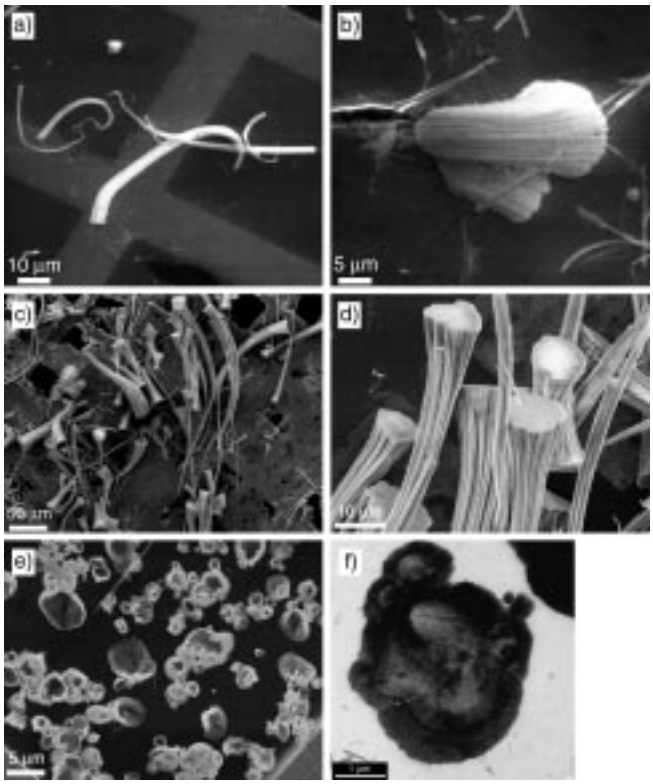


Figure 7. $BaSO_4$ crystallised in the presence of PEG-*b*-PMAA-$PO_3H_2$ on carbon films. a,b) Fibres with an ageing time of one and five days (c,d). e,f) $BaSO_4$ hollow cones after an ageing time of five days. See text for details.

widened to a rather flat terminating tip, such that the bundled structure had the shape of a highly elongated cone. Moreover, the large fibres became curved and grew back towards the substrate, presumably due to increasing weight (Figure 7b). After five days, many bundles of nanofilaments with lengths up to several hundred micrometers lay across the copper grid (Figure 7c). Evidently, some bundles were still in place but most were disrupted during sample preparation. The ends of the bundles were capped with a well-defined flat and uniform growth edge (Figure 7d) and smaller sub-bundles emanated from the sides of the pre-formed fibre leading to divergent growth. This observation suggests that the widening of the bundles towards the growth edge takes place through the secondary nucleation, and growth of new sub-bundles on the side surfaces of the existing structure near the growth tips, which is consistent with the finding that the individual nanofilaments constituting the bundles are essentially unchanged in thickness while developing in length. TEM images confirmed that the thickness of the nanofilaments was between 20 to 30 nm, which was very similar to those observed in the $BaSO_4$ bundles produced in glass tubes (Figure 5b).

Finally, after five days of ageing, micrometer-sized hollow cones consisting of $BaSO_4$ nanofilaments were also observed on the TEM grids. As shown in Figure 7 e,f, the randomly distributed cones nucleated on the carbon support film and splayed outwards into the solution. Their hollow-cone morphology clearly shows similarity to the results obtained with polyacrylate. Considering that no such hollow fibrous cones were observed at the earlier stages of growth, their formation is presumably associated with reduced levels of the amorphous $BaSO_4$ precursor nanoparticles in the solution. Under these conditions, the formation of empty fibrous cones rather than bundles of densely co-aligned nanofilaments would be favoured.

## Conclusion

Herein we have shown that aqueous solutions of a relatively low molecular mass polyacrylate or partially monophosphonated poly(ethyleneoxide)-block-polymethacrylate can be used to produce bundles or cones of highly anisotropic $BaSO_4$ nanofilaments by slow transformation of amorphous precursor particles. Similar results were previously observed for the formation of coiled and twisted bundles of $BaSO_4$[30] and $BaCrO_4$[31] nanofilaments in AOT water-in-oil microemulsions, suggesting that a general mechanism is responsible for these unusual morphological forms.

In each system studied, the nucleation and stabilisation of amorphous nanoparticles seems to be essential for nanofilament growth. Because both polymers bind $Ba^{2+}$ ions in solution (data not shown), nucleation of the amorphous $BaSO_4$ phase is associated with the extraction of $Ba^{2+}$ ions bound to the polymer side chains. (A similar mechanism occurs for the AOT system in which the $Ba^{2+}$ ions are strongly associated with the sulfonate headgroups of the surfactant prior to nucleation). Reaction with $SO_4^{2-}$ ions therefore occurs in close proximity to the polymer molecules, which adsorb onto the surface of the nuclei, thereby preventing crystallisation and arresting growth. The block copolymer, which is known to be a strong inhibitor of $BaSO_4$ nucleation due to the phosphonate groups,[29, 32–34] has a higher binding affinity than polyacrylate due to the increased acidity of the phosphonate groups and is therefore active even at low polymer concentrations. Polyacrylate, in contrast, is only active within a relatively narrow range of supersaturation values and $Ba^{2+}$:polymer molar ratios with relatively high polymer concentrations. Moreover, the block structure of PEG-b-PMAA-$PO_3H_2$ may increase the stabilisation of the amorphous precursor particles due to the separation of the binding polyelectrolyte moiety and stabilising PEG block[23] compared with the homopolymer structure of polyacrylate. Consequently, the higher concentration of amorphous particles gives rise to solid fibres and cones rather than the hollow structures observed in the presence of polyacrylate.



0947-6539/01/0716-3530 $ 17.50+.50/0 *Chem. Eur. J.* **2001**, *7*, No. 16

Figure 8 summarises a possible mechanism for the development of the bundles of $BaSO_4$ nanofilaments from the amorphous precursor particles. The mechanism is in part similar to that suggested for the formation of $BaSO_4$ nanofilaments in AOT microemulsions[30] except that attractive hydrophobic interactions between the AOT tails are replaced by attractive van der Waals forces operating between the colloids. Initially, the polymer-stabilised amorphous particles (stage 1, Figure 8) aggregate into colloidal clusters (stage 2, Figure 8) presumably due to van der Waals interactions between the particles. As the polyacrylate homopolymer chains are relatively small ($M_n = 5100\ g\,mol^{-1}$) and the PEO block is only $5000\ g\,mol^{-1}$, these interactions are likely to be sufficient to offset the accompanying steric repulsion. Crystallisation of $BaSO_4$ nanoparticles then occurs in the aggregates (stage 3, Figure 8) as the amorphous precursors are in close proximity and the lattice energy is increased and surface area reduced by particle fusion and structural rearrangement. At the same time, the anionic polymer chains adsorb selectively to positively charged crystal faces. We speculate that the presence of different charges on various faces as well as different shielding factors of the faces due to polymer adsorption leads to the formation of an electrostatic multipole field (stage 4, Figure 8), which directs the aggregation of the crystalline $BaSO_4$ building blocks along one principal axis to produce the nanofilament (stages 5 and 6, Figure 8). In support of this electric dipole field-induced vectorial process, we note that long fresnoite needles were deposited during the electric field-induced crystallisation from a glass melt with their polar *c* axis oriented parallel to the electric field lines.[35] In principle, the multipole field should be tuneable by selective polyelectrolyte adsorption onto specific crystal faces and this might explain why different polymers give rise to fibre growth along different crystallographic axes—for example, nanofilaments are elongated along the [010] [1$\bar{2}$0] or [001] axis for polyacrylate, PEG-b-PMAA-$PO_3H_2$ and polymaleate,[21] respectively.

Although the exact reason for uni-directional particle fusion is not yet clear, the experimental results indicate that it proceeds with high fidelity as the nanofilaments grow defect-free up to several tens of micrometres in length. This is in contrast to filament growth that is driven by selective blocking of growth faces, which often results in defects being expressed as branched outgrowth.[27] The filaments have a uniform width throughout their length which implies that the thickness is controlled at the initial stages of crystallisation and the side faces are blocked from growth by polymer adsorption. This was consistent with thermogravimetric analysis (TGA) of the nanofilaments grown in solution in the presence of the phosphonated block copolymer, which assuming a filament diameter of 25 nm, a length of 100 μm, $\rho_{BaSO4} = 4.5\ g\,mL^{-1}$ and $\rho_{Polymer} = 1.2\ g\,mL^{-1}$, gave a polymer content of 8.8 wt%, corresponding to a 4 nm-thick polymer layer around each filament.

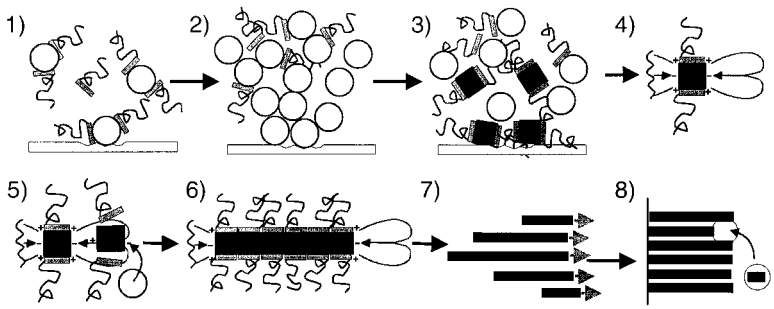


Figure 8. Proposed model for the heterogeneous nucleation and growth of fibre bundles.

In most structures, uni-directional crystallisation occurs in primary aggregates deposited on the walls of the reaction vessel so that the nanofilaments are asymmetric and grow from one end only. With time, secondary nucleation on the side surfaces produces bundles of co-aligned nanofilaments that are probably held together by attractive van der Waals forces and crystal multipole forces. However, although the filaments are crystallographically coherent, the extent of fusion is minimal and individual nanofilaments can be observed when the bundles are sectioned perpendicular to the growth axis.[29] This suggests that a repulsive steric layer of intercalated polymer molecules lies between the nanofilaments throughout the fibre in agreement with the above calculation based on the TGA result.

Because secondary nucleation occurs near the single growth edge, the bundles widen as they increase in length (step 7, Figure 8). Moreover, the bundles twist and coil as they increase in size, and become splayed into cone-shaped structures, particularly when the amount of polymer present becomes significantly reduced by intercalation into the growing bundles. The remarkably flat growth edges of the fibres displayed in Figure 7d suggests that residual amorphous precursor nanoparticles in solution are continually attracted to the growth front so that propagation of the bundle is by reaction-limited aggregation (stage 8, Figure 8), which minimises the surface energy. This means that the tips grow layer by layer preserving the flat surface by transport and controlled attraction of amorphous $BaSO_4$ nanoparticles. In contrast, when the level of nanoparticles is reduced, for example in the presence of the less-active polyacrylate molecules, hollow bundles and cones are produced.

In conclusion, the production of brush-like, cone-shaped, and multiple-cone-shaped fibrous $BaSO_4$ particles and well-defined bundles of $BaSO_4$ nanofilaments at room temperature in aqueous solutions of anionic polymers represents a useful route to the biomimetic synthesis of inorganic structures with complex form. The defect-free growth of filaments over several length scales in aqueous solution provides a good example of using cooperative structure-directing forces in materials synthesis. Although these forces have yet to be fully elucidated, their potential is clear. It should be possible to extend the experimental procedures to other inorganic systems, and this will be the subject of further work.

## Experimental Section

Sodium polyacrylate ($M_n = 5100\ g\,mol^{-1}$, $M_w/M_n \approx 3$) was purchased from Fluka. Each molecule was of mixed configuration (syndiotactic, isotactic and atactic). On average (based on $M_n$), a single chain comprised 50–60 acrylate subunits. The sodium content of the polymer was reported by the manufacturer to be 19% w/w, implying that only a minority of the carboxyl groups were protonated. For the average $pK_a$ value the literature value of 5.8 to 6.4 was assumed .[36] The block copolymer poly(ethyleneglycol)-*block*-poly(methacrylic acid) (PEG-*b*-PMAA, PEG = 3000 g mol$^{-1}$, 68 monomer units, PMAA = 700 g mol$^{-1}$, 6 monomer units) was obtained from Th. Goldschmidt AG, Essen, Germany. The carboxylic acid groups of this copolymer were partially monophosphonated (21%) to give a copolymer with phosphonate groups, PEG-*b*-PMAA-$PO_3H_2$.[25] The copolymer was purified by exhaustive dialysis before use as a crystal growth additive.

Barium sulfate crystals were prepared in the presence of an aqueous solution of polyacrylate as follows. Stock solutions of the polyacrylate were made, and aliquots of these were added to barium chloride and sodium sulfate solutions, prior to mixing, to give final polymer concentrations of 0.11 or 0.53 mM (with respect to acrylate subunits). The solutions were mixed to give supersaturation ratios of 60:1 to 170:1 ($[BaSO_4] = 1.0$ to 5.0 mM) at [acrylate] = 0.11 mM, and S = 60 to 220 ($[BaSO_4] = 1.0$ to 7.5 mM) at [acrylate] = 0.53 mM. The corresponding $BaSO_4$:acrylate molar ratios were between 9 to 45:1, and 1.9 to 14:1, respectively. Each reaction was performed using equal concentrations of barium and sulfate ions and was maintained unstirred at a constant temperature of 25 °C and a final pH of 5.8 for several weeks. The solution supersaturation ($S = \{[IAP/K_{sp}]\}^{0.5}$, where IAP = the ionic activity product and $K_{sp}$ = solubility product ($1.09 \times 10^{-10}$ mol$^2$ l$^{-2}$), was calculated using the computer program IONPRODUCT.[37] In the case of sodium polyacrylate, the input data was adapted to take into account $Ba^{2+}$ – -polyacrylate complexation. Previous studies[38–40] as well as observations made in this work indicate that barium ions bind very strongly to polyacrylate molecules. At equimolar concentrations, a 1:2 barium:carboxyl group complex is formed. Therefore, the concentration of free barium ions was taken as the total concentration of barium ions minus half the concentration of acrylate subunits. The reproducibility of the obtained $BaSO_4$ morphologies is good.

High yields of fibre bundles of $BaSO_4$ nanofilaments were repeatedly prepared in the presence of the phosphonated (21%) copolymer PEG-*b*-PMAA-$PO_3H_2$ ($M \approx 4000$ g mol$^{-1}$) at pH 5. A solution of 30 mg PEG-*b*-PMAA-$PO_3H_2$ in water (30 mL) was prepared (c = 0.25 mM) and adjusted to pH 5 by using 0.1 M HCl. Then, 0.05 M $Na_2SO_4$ (1.2 mL; Sigma, 99%) and 0.05 M $BaCl_2$ (1.2 mL; BDH Chemical Ltd., 99%) were added successively under vigorous stirring at room temperature, resulting in a final $BaSO_4$ concentration of 2 mM. After 2 min of stirring, the resulting transparent solution was poured into either plastic vessels or glass tubes and allowed to stand under quiescent conditions. Portions of the solution were poured into several 5 mL glass tubes and TEM and SEM samples were prepared by placing a drop of the solution after sonication for 3 min onto copper TEM grids and SEM stubs, respectively. Samples were taken after 24 h of mixing unless otherwise specified. In some experiments, aliquots of the solution were poured into a series of 1.5 mL polypropylene tubes (Plastibrand), each containing a carbon-coated, Formvar-covered, copper TEM grid (3 mm in diameter) at the bottom of the tube with the carbon film exposed to the solution. The copper grids were removed from the solution after various time intervals, allowed to dry in air, and then directly used for TEM and SEM characterisation.

## Acknowledgements

The Max-Planck Society and the University of Bristol are acknowledged for financial support. We also thank the DAAD and the British research council for travel funding (ARC grant). H.C. acknowledges financial support by the Dr. Hermann Schnell foundation. Th. Goldschmidt AG, Essen is acknowledged for the PEG-*b*-PMAA block copolymer.

[1] X. Peng, L. Manna, W. Yang, J. Wickham, E. Scher, A. Kadavanich, A. P. Alivisatos, *Nature* **2000**, *404*, 59–61.
[2] X. Duan, C. M. Lieber, *Adv. Mater.* **2000**, *12*, 298–302.
[3] J. D. Holmes, K. P. Johnston, R. C. Doty, B. A. Korgel, *Science* **2000**, *287*, 1471–1473.
[4] S. Fan, M. G. Chapline, N. R. Franklin, T. W. Tombler, A. M. Cassell, H. Dai, *Science* **1999**, *283*, 512–514.
[5] G. Che, B. B. Lakshmi, E. R. Fisher, C. R. Martin, *Nature* **1998**, *393*, 346–349.
[6] D. Xu, Y. Xu, D. Chen, G. Guo, L. Gui, Y. Tang, *Adv. Mater.* **2000**, *12*, 520–522.
[7] W. Wang, Y. Geng, Y. Qian, M. Ji, X. Liu, *Adv. Mater.* **1998**, *10*, 1479–1481.
[8] Y. Q. Zhu, W. B. Hu, W. K. Hsu, M. Terrones, N. Grobert, T. Karali, H. Terrones, J. P. Hare, P. D. Townsend, H. W. Kroto, D. R. M. Walton, *Adv. Mater.* **1999**, *11*, 844–847.
[9] V. M. Cepak, C. R. Martin, *J. Phys. Chem. B* **1998**, *102*, 9985–9990.
[10] Z. Zhang, D. Gekhtman, M. S. Dresselhaus, J. Y. Ying, *Chem. Mater.* **1999**, *11*, 1659–1665.
[11] M. P. Pileni, B. W. Ninham, T. Gulik-Krzywicki, J. Tanori, I. Lisiecki, A. Filankembo, *Adv. Mater.* **1999**, *11*, 1358–1362.
[12] P. D. Yang, C. M. Lieber, *Science* **1996**, *273*, 1836–1840.
[13] Y. Li, Meng. Sui, Y. Ding, G. Zhang, J. Zhuang, C. Wang, *Adv. Mater.* **2000**, *12*, 818–821.
[14] M. P. Pileni, T. Gulik-Krzywicki, J. Tanori, A. Filankembo, J. C. Dedieu, *Langmuir* **1998**, *14*, 7359–7363.
[15] J. D. Hopwood, S. Mann, *Chem. Mater.* **1997**, *9*, 1819–1828.
[16] L. Qi, J. Ma, H. Cheng, Z. Zhao, *J. Phys. Chem. B* **1997**, *101*, 3460–3463.
[17] G. D. Rees, R. Evans-Gowing, S. J. Hammond, B. H. Robinson, *Langmuir* **1999**, *15*, 1993–2002.
[18] K. Esumi, K. Matsuhisa, K. Torigoe, *Langmuir* **1995**, *11*, 3285–3287.
[19] M. B. Mohamed, K. Z. Ismail, S. Link, M. A. El-Sayed, *J. Phys. Chem. B* **1998**, *102*, 9370–9374.
[20] I. E. Brase, United States Patent, **1990**, number 4, 898, 677.
[21] W. J. Benton, I. R. Collins, I. M. Grimsey, G. M. Parkinson, S. A. Roger, *Faraday Discuss.* **1993**, *95*, 281–297.
[22] M. Sedlak, M. Antonietti, H. Cölfen, *Macromol. Chem. Phys.* **1998**, *199*, 247–254
[23] H. Cölfen, *Macromol. Rapid Commun.* **2001**, *22*, 219–252.
[24] J. M. Marentette, J. Norwig, E. Stöckelmann, W. H. Meyer, G. Wegner, *Adv. Mater.* **1997**, *9*, 647–651.
[25] H. Cölfen, M. Antonietti, *Langmuir* **1998**, *14*, 582–589.
[26] H. Cölfen, L. Qi, *Chem. Eur. J.* **2001**, *7*, 106–116.
[27] M. Antonietti, M. Breulmann, C. G. Göltner, H. Cölfen, K. K. W. Wong, D. Walsh, S. Mann, *Chem. Eur. J.* **1998**, *4*, 2493–2500.
[28] L. Qi, H. Cölfen, M. Antonietti, *Angew. Chem. Inter. Ed.* **2000**, *39*, 604–607.
[29] L. Qi, H. Cölfen, M. Antonietti, *Chem. Mater.* **2000**, *12*, 2392–2403.
[30] M. Li, S. Mann, *Langmuir* **2000**, *16*, 7088–7094.
[31] M. Li, H. Schnablegger, S. Mann, *Nature* **1999**, *402*, 393–395.
[32] J. D. Hopwood, PhD thesis, University of Bath, **1996**.
[33] L. A. Bromley, D. Cottier, R. J. Davey, B. Dobbs, S. Smith, B. R. Heywood; *Langmuir* **1993**, *9,* 3594–3599.
[34] M. C. van der Leeden, G. M. van Rosmalen, *J. Colloid Interface Sci.* **1995**, *171,* 142–149.
[35] R. Keding, C. Russel; *Phys. Chem. Chem. Phys.* **1996**, *100,* 1515–1518.
[36] C. Zhien-Chi, T. A. Ring, J. Lemaitre, *J. Am. Ceram. Soc.* **1992**, *75*, 3201–3208.
[37] R. P. Shellis, A microcomputer program to evaluate the saturation of complex solutions with respect to biominerals. CABIOS, IRL Press Limited, Oxford, England, **1988**, *4*, (3), 373–379.
[38] E. A. Bekturov, Z.Kh. Bakauova, *Synthetic water- soluble polymers in solution,* Huethig and Wepf, Heidelberg, Germany, **1986**, pp. 11–72.
[39] Z. Wojtczac, *J. Polym. Sci. A* **1965**, *3*, 3613.
[40] Z. Wojtczak, *Roczniki Chemi, Analytical Chemistry Society of Poland*, **1968**, *45*, 237.

Received: February 9, 2001 [F3061]

  0947-6539/01/0716-3532 $ 17.50+.50/0 